Published in final edited form as:
Circ Res. 2010 March 19; 106(5): 952–960. doi:10.1161/CIRCRESAHA.109.209007.

Modulation of Angiotensin II–mediated cardiac remodeling by the MEF2A target gene Xirp2

Sarah A. McCalmon, PhD[1], **Danielle M. Desjardins, BA**[1], **Saad Ahmad, MD**[2], **Katharine S. Davidoff**[1], **Christine M. Snyder, MA**[1], **Kaori Sato, MD**[2], **Koji Ohashi, MD, PhD**[2], **Ondra M. Kielbasa, MA**[1], **Matthen Mathew, BA**[1], **Elizabeth P. Ewen, MA**[1], **Kenneth Walsh, PhD**[2], **Haralambos Gavras, MD**[2,3], and **Francisco J. Naya, PhD**[1,2]

[1]Department of Biology, Program in Cell and Molecular Biology, Boston University, 24 Cummington Street, Boston, MA 02215

[2]Whitaker Cardiovascular Institute, Boston University Medical School, 700 Albany Street, Boston, MA 02118

[3]Alapis Research Laboratories, Boston University Medical School, 700 Albany Street, Boston, MA 02118

Abstract

Rationale—The vasoactive peptide angiotensin II (AngII) is a potent cardiotoxic hormone whose actions have been well studied, yet questions remain pertaining to the downstream factors that mediate its effects in cardiomyocytes.

Objective—The *in vivo* role of the MEF2A target gene *Xirp2* in AngII-mediated cardiac remodeling was investigated.

Methods and Results—Here we demonstrate that the MEF2A target gene *Xirp2* (also known as *cardiomyopathy associated gene 3; CMYA3*) is an important effector of the AngII signaling pathway in the heart. *Xirp2* belongs to the evolutionarily conserved, muscle-specific, actin-binding *Xin* gene family and is significantly induced in the heart in response to systemic administration of AngII. Initially, we characterized the *Xirp2* promoter and demonstrate that AngII activates *Xirp2* expression by stimulating MEF2A transcriptional activity. To further characterize the role of Xirp2 downstream of AngII signaling we generated mice harboring a hypomorphic allele of the *Xirp2* gene that resulted in a marked reduction in its expression in the heart. In the absence of AngII, adult *Xirp2* hypomorphic mice displayed cardiac hypertrophy and increased β*MHC* expression. Strikingly, *Xirp2* hypomorphic mice chronically infused with AngII exhibited altered pathological cardiac remodeling including an attenuated hypertrophic response, as well as diminished fibrosis and apoptosis.

Conclusions—These findings reveal a novel MEF2A-Xirp2 pathway that functions downstream of AngII signaling to modulate its pathological effects in the heart.

Address correspondence to Francisco J. Naya, Department of Biology, Boston University, 24 Cummington Street, Boston, MA 02215, Tel: 617-353-2469; Fax. 617-353-6340; fnaya@bu.edu.

Disclosures
None.

Keywords

Myocyte enhancer factor 2; Angiotensin II; Xirp2; myomaxin; cardiac hypertrophy; hypomorphic mice

Angiotensin II (AngII) is a potent hypertensive agonist that also promotes extensive myocardial damage even in the absence of hypertension (1). The repertoire of downstream effectors in AngII-mediated pathological cardiac remodeling, however, remains largely incomplete (2,3). A recent global gene expression study identified transcripts of a novel gene, named *CMYA3 (cardiomyopathy associated gene 3)*, that were up-regulated in hearts of mice treated with AngII but not in salt-induced hypertensive mice (4) suggesting that *CMYA3* is directly regulated by AngII signaling. This gene, since named *Xirp2* (also known as *mXin*β and *myomaxin*), is a direct target of the MEF2A transcription factor and is markedly down-regulated in hearts lacking MEF2A (5,6).

Xirp2 belongs to the ancient, muscle-specific, actin-binding *Xin* gene family whose expression can be traced to ancestral vertebrates with a two-chambered heart (7–9). Xirp2 is expressed in cardiac and skeletal muscle where it interacts with filamentous actin and α-actinin through the novel actin-binding motif, the Xin repeat (5,8). In striated muscle, Xirp2 localizes to the peripheral Z-disc region, or costamere (5), and the intercalated disk (10,11). The sub-cellular localization of Xirp2 is significant in that the costamere and intercalated disk harbor mechanical stress sensors that are critical for normal muscle function (12–14).

Antisense knockdown of *Xin* in developing chick embryos, the sole *Xin* family member in this species, results in a severe disruption of cardiac looping morphogenesis (9). In mice, a loss-of-function mutation of *mXin*α, the mammalian ortholog of *Xin*, results in cardiomyopathy and conduction defects (11). In the present study we sought to determine the role of *Xirp2* in cardiac development and/or function. Mice harboring a hypomorphic *Xirp2* allele are viable but display cardiac hypertrophy. As *Xirp2* is regulated by AngII, we also examined cardiac pathology in hypomorphic mice with long-term administration of this hormone. In contrast to wild type mice exposed to a chronic AngII infusion, hypomorphic mice displayed diminished cardiac hypertrophy, fibrosis, and apoptosis. Furthermore, we demonstrate that regulation of *Xirp2* gene expression in response to AngII signaling is mediated by MEF2A. Our results suggest that MEF2A and Xirp2 are important downstream effectors in mediating pathological cardiac remodeling in response to AngII signaling.

Methods

Details of materials and experimental procedures can be found in the expanded Methods section in the Online Data Supplement.

Generation of *Xirp2* loxP-targeted mice

Xirp2 loxP-neo targeted mice were generated by inGenious Targeting Laboratory Inc. (Stony Brook, NY).

Histology and immunofluorescence

Hearts were fixed in 4% paraformaldehyde, cryoprotected in sucrose, and placed in embedding compound (OCT). Whole-heart sections were stained with hematoxylin & eosin (H&E). Masson's trichrome staining was performed to determine the extent of cardiac fibrosis. Apoptosis was assessed by terminal dUTP nick-end labeling (TUNEL) assay using the Promega DeadEnd™ Colorimetric TUNEL System kit. For immunofluorescence, heart

cryosections were blocked in BSA prior to incubation with primary and secondary antibodies.

Administration of Angiotensin II

Angiotensin II (0.9μg/hr) was administered via subcutaneous osmotic mini-pumps (Alzet model 2004) for 14 days.

Echocardiography and blood pressure analysis

Transthoracic M-mode echocardiography was performed on mice at baseline (pre-treatment) and post-2week AngII infusion. Blood pressure analysis was performed using the non-invasive tail cuff method (Model BP 2000, Visitech Systems).

Microarray and gene expression analysis

cDNA was prepared from total RNA isolated from either hindlimb or ventricular tissue using Trizol reagent (Invitrogen). Primers for qRT-PCR/RT-PCR can be found in the Online Data Supplement. For qRT-PCR, individual non-pooled samples were run in triplicate wells. qRT-PCR was performed with SYBR® Green master mix (Applied Biosystems) using the 7900 Sequence Detection System (Applied Biosystems). For microarray, samples were prepared as described previously (15) and hybridized to the Mouse Gene 1.0 ST Array (Affymetrix) at the Boston University Microarray Facility.

Western blot analysis

To detect cardiac Xirp2 protein, ventricular muscle was snap-frozen in liquid nitrogen immediately following dissection, pulverized and resuspended in sample loading buffer. Protein concentrations were analyzed by Bradford assay. Samples were subjected to SDS-PAGE, transferred to PVDF membrane (Biorad) and immunoblotted using primary antibodies described in the Online Data Supplement.

Cell culture, luciferase assays, and plasmids

COS1 cells were grown in Dulbecco's modified Eagle medium with 10% Fetal Bovine Serum, 1% Penicillin/Streptomycin, and 1% L-Glutamine and transfected using Mirus TransIT®-LT1 transfection reagent. Luciferase assays were performed using Luciferase Assay Reagent (Promega), and results were normalized by Bradford assay. For analysis of Xirp2 expression in primary neonatal rat ventricular myocytes (NRVMs), cells were isolated as described previously (5). All *Xirp2* luciferase promoter constructs were cloned into the pGL3b-luciferase vector (Promega) except the −1425/−285 deletion mutant which was cloned into the pGL3p-luciferase construct (Promega).

Statistical analysis

Appropriate data sets were analyzed for significance using 2-way ANOVA. Variance of data sets was determined using the Bartlett's-test. Either a 2-tailed Student's t-test or Welch's t-test was performed for each pair-wise comparison. A p-value of <0.05 was considered to be statistically significant.

Results

AngII stimulates MEF2A transcriptional activity to regulate *Xirp2* expression

To determine whether the AngII-mediated up-regulation of *Xirp2* was a direct effect of the hormone on cardiomyocytes or due to secondary effects resulting from pressure overload, primary neonatal rat ventricular myocytes (NRVMs) were isolated and treated with AngII.

As shown in Figure 1A, *Xirp2* transcripts were induced in NRVMs upon AngII treatment indicating that *Xirp2* is directly stimulated by the hormone.

The above results prompted us to map the AngII-responsive region in the proximal 1.5kb *Xirp2* promoter (5). Due to the very high basal activity of this promoter and smaller deletion constructs in NRVMs, we were unable to detect enhanced activation by AngII in this system. Subsequently, we examined the responsiveness of various *Xirp2* promoter constructs (Fig. 1B) to AngII in COS cells since these cells express the type I angiotensin receptor. In transiently transfected COS cells, the −1425 *Xirp2* promoter was stimulated 2.5-fold by AngII (Fig. 1C). A truncated *Xirp2* promoter (−285/+60) was similarly activated by AngII (Fig. 1C), indicating that the AngII-responsive region resides within the first 300 base pairs upstream of the transcription start site. This minimal region harbors an essential MEF2 site (5). Given that MEF2 activity is modulated by AngII in vascular smooth muscle (16,17) we reasoned that AngII-induced *Xirp2* expression is mediated by MEF2. To test this hypothesis, we transfected a mutant promoter construct that harbors a mutation in the −75 MEF2 site (−285mut) which disrupts MEF2 DNA binding. AngII activation of the −285 mutant promoter was significantly reduced, indicating that the MEF2 site functions as an AngII-responsive element in the *Xirp2* promoter (Fig. 1C).

To further investigate the role of MEF2 downstream of AngII-mediated activation of the *Xirp2* gene, the −1425 *Xirp2* promoter was co-transfected in COS cells along with MEF2A in the presence or absence of AngII. AngII or MEF2A alone activated the −1425 promoter by 2.5-fold and 3.4-fold, respectively (Fig. 1D). The combination of AngII and MEF2A robustly activated the −1425 *Xirp2* promoter 10.6-fold (Fig. 1D). Similar results were observed with the −285 promoter construct (Fig. 1D). This cooperative effect was severely attenuated in three different mutant *Xirp2* promoters in which the −75 MEF2 site was either deleted (−1425/−285) or disrupted by point mutation (−1425mut and −285mut) (Fig. 1D). However, the ability of AngII to stimulate MEF2A was not mediated by enhanced binding to the MEF2 site (Online Fig. I).

To reinforce the notion that MEF2A is an essential regulator of *Xirp2* downstream of AngII signaling *in vivo*, we examined the expression of *Xirp2* in NRVMs in which MEF2A was knocked down by adenoviruses expressing MEF2A-specific short hairpin RNAs (shRNAs) (Online Fig. IX and to be described in detail elsewhere). We failed to observe an induction of *Xirp2* by AngII in cells transduced with MEF2A shRNAs but not control lacZ shRNAs (Fig. 1E, compare lanes 3 and 4 to lanes 5 and 6). These results demonstrate that *Xirp2* is a novel, direct transcriptional target of AngII whose induction is mediated by MEF2A.

Generation of *Xirp2* hypomorphic mice

Having established that *Xirp2* is directly regulated by AngII, we wanted to determine the *in vivo* requirement of this gene in AngII-induced cardiomyopathy. Therefore, we generated a conditional null allele of the *Xirp2* gene which contained loxP sequences flanking exons 4 and 6, and a PGK-neomycin (PGK-neo) cassette in the intron between exons 6 and 7 (Fig. 2A). To generate a complete loss-of-function allele, conditional *Xirp2* mice were crossed to EIIa-Cre transgenic mice which removed exons 4–6 along with the loxP flanked PGK-neo cassette in the germline. These heterozygous *Xirp2* loxP mice (+/loxP) were intercrossed resulting in homozygous *Xirp2* loxP/loxP mice that were viable, fertile and genotyped at the expected Mendelian ratios. The excision of exons 4–6 was confirmed by RT-PCR analysis on cardiac muscle cDNA (Fig. 2B). Sequencing of these truncated cDNAs revealed an in-frame splice between exons 3 and 7 (Fig. 2B). This in-frame splice had no effect on *Xirp2* expression in homozygous loxP/loxP mice (data not shown) and as a result, these mice have not been further characterized.

In parallel, we generated loxP-neo targeted *Xirp2* homozygous mice (referred to as loxP-neo) that retained the PGK-neo cassette (Fig. 2A). Homozygous loxP-neo mice were identified in the expected Mendelian ratios demonstrating that this allele, like the in-frame deletion, does not affect viability. As retention of PGK-neo can often interfere with expression of the targeted gene (18), we examined *Xirp2* transcript levels in homozygous loxP-neo mice by quantitative real time RT-PCR (qRT-PCR). Using primers spanning exons 2 and 3, qRT-PCR analysis of cardiac and skeletal muscle cDNA revealed that these tissues express *Xirp2* at only 15–20% of wild type levels (Fig. 2C). RT-PCR analysis using multiple downstream primer sets demonstrated similar results suggesting that full length *Xirp2* transcripts are being produced from the loxP-neo targeted allele (Online Fig. II). In addition, Xirp2 protein is largely absent from both hindlimb and cardiac muscle extracts (Fig. 2D). Unlike the up-regulation of *Xirp2* in *Xin* knockout hearts (11), there was no compensatory increase in *Xin* gene expression in *Xirp2* hypomorphic hearts (Fig. 2E). Given these exciting results we focused on characterizing the cardiac phenotype of *Xirp2* hypomorphic mice.

Cardiac hypertrophy in *Xirp2* hypomorphic mice

Because Xirp2 is enriched at the muscle costamere we reasoned that its reduction would adversely affect the normal growth and/or function of the heart. We measured heart weight : body weight (HW:BW) ratios in wild type and *Xirp2* hypomorphic adult mice. Between 9 and 15 weeks post-natally *Xirp2* hypomorphic mice displayed a modest increase in HW:BW ratio (19%) (Fig. 3A). We performed morphometric analysis of ventricular myocytes in adult hypomorphic hearts and observed a significant increase in the cross-sectional area (CSA) (1.6-fold) (Fig. 3B) but other hallmarks of cardiomyopathy such as fibrosis and apoptosis were not significantly altered (data not shown). Similarly, examination of cardiomyocytes by electron microscopy did not reveal any obvious perturbations in myofibrillar structure (data not shown). Echocardiographic assessment of cardiac function showed no significant differences in ejection fraction (%EF) or fractional shortening (%FS) in hypomorphic mice (Online Fig. III). As Xirp2 is also expressed in skeletal muscle future studies will focus on the characterization of a possible phenotype in this tissue.

To further characterize the hypertrophic phenotype we examined the expression of hypertrophic marker genes by qRT-PCR. There was no significant change in expression of atrial natriuretic factor (*ANF*), brain natriuretic peptide (*BNP*), or alpha myosin heavy chain (α*MHC*) genes (Fig. 4A). However, *Xirp2* hypomorphic hearts exhibited a significant activation (3.9-fold) of the beta myosin heavy chain (β*MHC*) gene (Fig. 4A).

Global dysregulation of cardiac gene expression in *Xirp2* hypomorphic mice

To investigate the molecular mechanisms of the hypomorphic cardiac phenotype we performed microarray analysis of ventricular RNA from adult wild type and *Xirp2* hypomorphic mice. We found a dysregulation of genes belonging to a broad spectrum of functional categories including metabolism (15%), muscle contraction (11%), calcium handling (9%), and cytoskeleton (5%) (Fig. 4B). A subset of these genes was validated by qRT-PCR. *MARCKS* (*myristoylated alanine-rich C kinase substrate*), *Pdlim3/ALP* (α-*actinin interacting LIM protein*), and *Lipocalin 2* genes were significantly up-regulated, whereas *RCAN1/MCIP1* (*regulator of calcineurin*) was significantly down-regulated (Fig. 4C). In addition, the down-regulation of RCAN1/MCIP1 was confirmed by Western blot analysis (Online Fig. IV). Interestingly, like Xirp2, both MARCKS and Pdlim3/ALP are involved in F-actin and α-actinin cross-linking dynamics, respectively (19,20). The *Lipocalin 2* gene encodes a glycoprotein involved in numerous cellular processes (21) and its up-regulation in hypomorphic hearts is consistent with the reported activation of this gene in human and rodent models of heart failure (22). One possible outcome of reduced RCAN1/MCIP1, a modulator of the pro-hypertrophic factor calcineurin (23), is an elevation in

calcineurin activity, and consequently, increased cardiomyocyte size in hypomorphic hearts. Taken together, the above data are consistent with pathologic cardiac hypertrophy in *Xirp2* hypomorphic mice.

Diminished cardiac pathophysiology in *Xirp2* hypomorphic mice infused with AngII

To determine whether Xirp2 is required for stress-induced cardiac remodeling *in vivo* we subjected hypomorphic mice to chronic AngII infusion. The 2-week AngII infusion in wild type mice resulted in a 20% increase in HW:BW (Fig. 5A) which was confirmed by the 2.5-fold increase in ventricular myocyte CSA (Fig. 5B). In contrast, AngII treatment failed to induce a significant increase in HW:BW ratios in AngII-infused hypomorphic mice (Fig. 5A). This evidence of attenuated cardiac hypertrophy is supported by the less pronounced increase in hypomorphic cardiomyocyte CSA compared to that of wild type animals (1.7-fold compared to 2.7-fold respectively) (Fig. 5B). These results indicate that the residual amount of Xirp2 in hypomorphic hearts is insufficient to fully induce the hypertrophic effects of AngII.

Since chronic AngII administration induces cardiac interstitial fibrosis, we subjected hearts from wild type and hypomorphic mice to Masson's trichrome staining. Upon treatment with AngII, wild type mice exhibited a 2.8-fold increase in fibrosis relative to sham-operated animals (Fig. 5C). In striking contrast, chronic AngII infusion was unable to stimulate an increase in fibrosis in *Xirp2* hypomorphic mice (Fig. 5C). We subsequently performed TUNEL assay to assess the extent of apoptosis in AngII-infused hearts. AngII-infused wild type mice showed a 3.3-fold increase in the amount of TUNEL-positive cells in the heart (Fig. 5D). However, AngII-infused *Xirp2* hypomorphic mice showed no significant increase in myocardial apoptosis (Fig. 5D). Finally, the AngII dose used in this study induced hypertension in wild type and hypomorphic mice without any significant difference between the two groups (Online Fig. V).

Analysis of hypertrophic markers in *Xirp2* hypomorphic mice upon AngII infusion

Given the dampened cardiomyopathy in AngII treated hypomorphic mice we examined the expression of hypertrophic markers in hearts with long term administration of AngII. Wild type animals displayed an increase in β*MHC* (5.7-fold) and *ANF* (5.1-fold) expression (Fig. 6A). In contrast, β*MHC* expression was not significantly increased in *Xirp2* hypomorphic hearts upon AngII-infusion, whereas *ANF* displayed responsiveness to AngII. Expression of α*MHC* and *BNP* was not significantly dysregulated in either wild type or hypomorphic hearts upon AngII-infusion (Fig. 6A). These results show a differential response of β*MHC* to AngII signaling in stressed hypomorphic hearts which correlates with attenuated cardiac hypertrophy in these animals.

To further understand the mechanisms behind the attenuated cardiomyopathy in stressed hypomorphic mice we examined phosphorylation levels of intracellular signaling molecules known to function downstream of AngII. By Western blot analysis, we found no significant difference in the phosphorylation of the MAPK components, Erk1/2, p38, and JNK, or protein kinase D1 (PKD1) (24) in AngII-infused hypomorphic hearts (data not shown). Also, we found no difference in the transcript or protein levels of the type I Angiotensin receptor (AT1R) (Online Fig. VI). In contrast, GSK-3β serine-9 phosphorylation was significantly reduced in AngII-infused *Xirp2* hypomorphic hearts (Fig. 6B). This effect does not appear to be mediated by Akt, an upstream kinase of GSK-3β, since Western blot analysis did not detect differences in its activity in hypomorphic hearts (Online Fig. VII). Inhibition of GSK-3β kinase activity, a well established hypertrophic antagonist, through increased phosphorylation on serine-9, is associated with enhanced hypertrophy (25). A major target of active GSK-3β is β-catenin, which is phosphorylated by GSK-3β and is

subsequently targeted for ubiquitination and degradation (26). Western blot analysis revealed that β-catenin levels are significantly diminished in AngII-treated hypomorphic mice (Fig. 6C). Thus, the reduction in GSK-3β serine-9 phosphorylation in AngII-treated hypomorphic mice is consistent with diminished cardiac hypertrophy.

Discussion

In the present study we report for the first time that the novel MEF2A target gene, *Xirp2*, is an essential mediator of AngII-induced pathological cardiac remodeling *in vivo*. We generated a *Xirp2* hypomorphic allele which resulted in a marked reduction in its expression in skeletal and cardiac muscle in mice. Although these mice are viable, unstressed *Xirp2* hypomorphic mice display cardiac hypertrophy. Paradoxically, hearts from hypomorphic mice infused with AngII displayed attenuated cardiac hypertrophy, interstitial fibrosis and cardiomyocyte apoptosis.

It is well documented that AngII promotes myocardial damage, thus the identification of novel mediators of this signaling pathway in the heart is an important goal. We now provide evidence that *Xirp2* is a direct transcriptional target of AngII signaling in cardiac muscle. Further, the activation of the *Xirp2* gene by AngII is controlled, in part, by the MEF2A transcription factor. The related *Xin* gene is also a MEF2 target (9) yet expression of this gene was not significantly induced in the heart by AngII. These observations suggest a tightly controlled regulation of the *Xin* gene family involving the AngII signaling pathway and MEF2.

By generating mice with a hypomorphic *Xirp2* allele we were able to establish that Xirp2 is required for the proper physiological growth of the heart, since a reduction in its expression resulted in enlarged cardiomyocyte size. Cardiac hypertrophy in hypomorphic mice was accompanied by an up-regulation of the hypertrophic marker gene, β*MHC*, and a down-regulation of the calcineurin modulatory gene, *RCAN1/MCIP1*. The down-regulation of a calcineurin modulator provides a plausible mechanism by which unstressed hypomorphic mice develop myocyte hypertrophy through increased calcineurin activity (27). Furthermore, the upregulation of *Pdlim3/ALP* and *MARCKS*, which encode cytoarchitectural proteins involved in actin dynamics localized to costameres and focal adhesions, respectively, may indicate a compensatory response to the reduction of Xirp2 at these structures. The cardiac phenotype displayed by unstressed *Xirp2* hypomorphic mice is reminiscent of *Xin* knockout mice which also develop adult onset hypertrophy (11). These findings suggest that Xirp2 and Xin have partially overlapping functions in unstressed cardiomyocytes. In the future it will be of interest to determine the consequences in cardiac development and/or function in mice lacking both Xin family members.

The up-regulation of the hypertrophic marker, β*MHC*, but not other fetal cardiac genes in unstressed *Xirp2* hypomorphic mice suggests an unconventional, but not unprecedented, mechanism of pathologic cardiac remodeling. Transgenic mice overexpressing either the beta2 adrenergic receptor (β_2AR) or an inhibitor of beta adrenergic receptor kinase 1 (βARK1ct) in the heart displayed elevated levels of the β*MHC* but not the *ANF* or *skeletal α-actin* genes (28). While the significance of this specific pattern of hypertrophic gene dysregulation is not entirely clear these observations reveal that the coordinate up-regulation of fetal cardiac genes is not a universal pathway and does not apply to all models of cardiomyopathy.

Our data also reveal an attenuation of AngII-induced pathological cardiac remodeling in *Xirp2* hypomorphic mice. The attenuated hypertrophy, fibrosis, and apoptosis were accompanied by compromised activation of β*MHC* expression and reduced phosphorylation

of GSK-3β and thus reduced β-catenin levels. Expression of the β*MHC* gene is sensitive to cardiac stress (29), and the failure to further up-regulate β*MHC* expression in AngII treated hypomorphic mice is likely a direct indication of the diminished hypertrophy. It is known that active GSK-3β functions as a hypertrophic antagonist and that phosphorylation of the kinase at serine-9 is an inactivating modification (25,26). It follows that expression of an un-phosphorylatable form of GSK-3β (GSK-3βS9A) in cardiomyocytes suppresses hypertrophy (30,31). Thus, reduced GSK-3βS9 phosphorylation in AngII treated hypomorphic mice may provide a mechanism for the dampened cardiac hypertrophy. Further, the concomitant reduction in β-catenin levels in AngII-treated hypomorphic hearts is consistent with reports that depletion or reduction of β-catenin in the heart results in blunted pathological cardiac remodeling in response to stress (32,33).

The reduced fibrosis and apoptosis in AngII treated hypomorphic mice demonstrates that *Xirp2* is required to promote these hallmarks of pathological remodeling in the heart downstream of this hormone. These results provide the first evidence that Xirp2 may be involved in cell survival pathways in cardiac stress signaling. As myocyte cell death and interstitial fibrosis are major contributors to end stage heart failure, minimizing the extent of these abnormalities in the diseased heart would be expected to significantly improve cardiac function. It is tempting to speculate that modulating Xirp2 expression through pharmacological strategies could identify an optimal level of Xirp2 activity that does not induce hypertrophy under normal physiological conditions but blunts pathologic cardiac remodeling in response to stress.

Surprisingly, the pre-existing cardiac hypertrophy in unstressed hypomorphic mice was not exacerbated by long-term administration of AngII. The attenuated cardiac remodeling in AngII treated hypomorphic mice may point to a unique, additional role for Xirp2 in the modulation of AngII signals that is not dependent on, and largely separable from, its basal function in cardiac development and homeostasis. In support of this hypothesis, microarray analysis on AngII treated hypomorphic mice (Online Fig. VIII) revealed that the global profile of dysregulated genes in unstressed hypomorphic mice was largely distinct from the dysregulated gene program in AngII treated hypomorphic mice (hypo vs. AngII-hypo). These data argue against a common gene program triggered by the reduction of Xirp2 in the absence and presence of cardiac stress.

Collectively, our data support the notion that Xirp2 possesses two distinct functions in cardiomyocytes, such that its reduced levels in unstressed conditions is deleterious to the heart, but in the presence of stress, limiting amounts of Xirp2 appear to be beneficial. We previously reported that *Xirp2* expression in NRVMs is induced by additional hypertrophic stimuli such as phenylephrine and serum (5). Therefore, it will be important to investigate whether a reduction in Xirp2 can also influence cardiac remodeling in response to additional neurohormonal insults and biomechanical stressors, or whether Xirp2 functions specifically as a mediator of AngII-induced cardiomyopathy.

Novelty and Significance

What is known?

- The hormone angiotensin II has widespread damaging effects on the heart but only a few downstream genes are known to mediate its effects.
- The muscle-specific, actin-binding Xirp2 gene is regulated by angiotensin II.
- The Xirp2 gene is regulated by the MEF2A transcription factor.

What new information does this article contribute?

- A novel mouse model with reduced expression of Xirp2 in the heart results in cardiac hypertrophy.
- Hearts with reduced Xirp2 expression display less myocardial damage when exposed to angiotensin II.
- Angiotensin II regulates Xirp2 through the MEF2A transcription factor.

In this manuscript we report that in the hear the evolutionarily conserved,actin-binding protein, Xirp2, functions downstream of angiotensin II (AngII) signaling

Prior to this report no information existed pertaining to the *in vivo* function of Xirp2 in the heart. To our knowledge this study is the first to describe the cardiac phenotype of a mouse knockdown model of *Xirp2*. We show that a reduction in Xirp2 expression in the heart results in pathologic cardiac hypertrophy in adult, unstressed mice. Interestingly, these mice display a blunted response to AngII-induced myocardial damage. This study demonstrates for the first time that the MEF2A target gene, *Xirp2*, plays an essential role in cardiomyocytes *in vivo* by mediating AngII-induced pathological cardiac remodeling. Furthermore, we demonstrate that the MEF2A transcription factor acts directly downstream of the AngII signaling pathway to regulate *Xirp2* gene expression. Our findings have broad implications regarding muscle-specific, actin-binding genes that modulate cardiac muscle function in health and disease.

Supplementary Material

Refer to Web version on PubMed Central for supplementary material.

Non-standard Abbreviations and Acronyms

MEF2A	myocyte enhancer factor 2A
Xirp2	Xin-repeat protein 2
CMYA3	cardiomyopathy associated gene 3
COS	kidney fibroblast cell line
shRNA	short hairpin RNA
hypo	hypomorphic
CSA	cross-sectional area
RCAN	regulator of calcineurin
GSK	glycogen synthase kinase

Acknowledgments

We are grateful to Jun Sadoshima (UMDNJ, Newark, NJ) for the total and phospho-S9-GSK-3β antibodies, Timothy McKinsey (Gilead, Westminster, CO) for the PKD1 antibodies, Jeffery Molkentin (HHMI, Cincinnati, OH) for MCIP1 antibodies, Isabel Dominguez (Boston University) for β-catenin antibodies, and Geoffrey Copper (Boston University) for total and phospho-Akt antibodies. We also thank Andrew Betts of Ubixum Inc. (Palo Alto, CA) for assistance with Matlab image processing and Susan Kandarian (Boston University) for use of Metamorph software.

Sources of Funding

This work was supported by a grant from the NIH/NHLBI and Muscular Dystrophy Association (F.J.N.), a Clare Boothe Luce Fellowship (S.A.M)., a post-doctoral NIH Cardiovascular Training Grant (S.A.), and undergraduate research fellowships from the American Heart Association to D.D and M.M., and a Boston University Undergraduate Research Opportunities (UROP) fellowship to K.D.

References

1. Gavras H, Brown JJ, Lever AF, Macadam RF, Robertson JIS. Acute renal failure, tubular necrosis, and myocardial infarction induced in the rabbit by intravenous angiotensin II. Lancet 1971;2:19–22. [PubMed: 4103665]
2. Kim S, Iwao H. Molecular and cellular mechanisms of angiotensin II-mediated cardiovascular and renal diseases. Pharmacol Rev 2000;52:11–34. [PubMed: 10699153]
3. Larkin JE, Frank BC, Gaspard RM, Duka I, Gavras H, Quackenbush J. Cardiac transcriptional response to acute and chronic angiotensin II treatments. Physiol Genomics 2004;18:152–166. [PubMed: 15126644]
4. Duka A, Schwartz F, Duka I, Johns C, Melista E, Gavras I, Gavras H. A novel gene (Cmya3) induced in the heart by angiotensin II-dependent but not salt-dependent hypertension in mice. Am J Hypertens 2006;19:275–281. [PubMed: 16500513]
5. Huang HT, Brand OM, Mathew M, Ignatiou C, Ewen EP, McCalmon SA, Naya FJ. Myomaxin is a novel transcriptional target of MEF2A that encodes a Xin related alpha-actinin-interacting protein. J Biol Chem 2006;281:39370–39379. [PubMed: 17046827]
6. Naya FJ, Black BL, Wu H, Bassel-Duby R, Richardson JA, Hill JA, Olson EN. Mitochondrial deficiency and cardiac sudden death in mice lacking the MEF2A transcription factor. Nat Med 2002;8:1303–1309. [PubMed: 12379849]
7. Grosskurth SE, Bhattacharya D, Wang Q, Lin JJ. Emergence of Xin demarcates a key innovation in heart evolution. PLoS ONE 2008;3:e2857. [PubMed: 18682726]
8. Pacholsky D, Vakeel P, Himmel M, Löwe T, Stradal T, Rottner K, Fürst DO, van der Ven PF. Xin repeats define a novel actin-binding motif. J Cell Sci 2004;117:5257–5268. [PubMed: 15454575]
9. Wang DZ, Reiter RS, Lin JL, Wang Q, Williams HS, Krob SL, Schultheiss TM, Evans S, Lin JJ. Requirement of a novel gene, Xin, in cardiac morphogenesis. Development 1999;126:1281–1294. [PubMed: 10021346]
10. Sinn HW, Balsamo J, Lilien J, Lin JJ. Localization of the novel Xin protein to the adherens junction complex in cardiac and skeletal muscle during development. Dev Dyn 2002;225:1–13. [PubMed: 12203715]
11. Gustafson-Wagner EA, Sinn HW, Chen YL, Wang DZ, Reiter RS, Lin JL, Yang B, Williamson RA, Chen J, Lin CI, Lin JJ. Loss of mXinalpha, an intercalated disk protein, results in cardiac hypertrophy and cardiomyopathy with conduction defects. Am J Physiol Heart Circ Physiol 2007;293:H2680–H2692. [PubMed: 17766470]
12. Clark KA, McElhinny AS, Beckerle MC, Gregorio CC. Striated muscle cytoarchitecture: an intricate web of form and function. Annu Rev Cell Dev Biol 2002;18:637–706. [PubMed: 12142273]
13. Samarel AM. Costameres, focal adhesions, and cardiomyocyte mechanotransduction. Am J Physiol Heart Circ Physiol 2005;289:H2291–H2301. [PubMed: 16284104]
14. Ervasti JM. Costameres: the Achilles' heel of Herculean muscle. J Biol Chem 2003;278:13591–13594. [PubMed: 12556452]
15. Durham JT, Brand OM, Arnold M, Reynolds JG, Muthukumar L, Weiler H, Richardson JA, Naya FJ. Myospryn is a direct transcriptional target for MEF2A that encodes a striated muscle, alpha-actinin-interacting, costamere-localized protein. J Biol Chem 2006;281:6841–6849. [PubMed: 16407236]
16. Suzuki E, Nishimatsu H, Satonaka H, Walsh K, Goto A, Omata M, Fujita T, Nagai R, Hirata Y. Angiotensin II induces myocyte enhancer factor 2- and calcineurin/nuclear factor of activated T cell-dependent transcriptional activation in vascular myocytes. Circ Res 2002;90:1004–1011. [PubMed: 12016267]
17. Suzuki E, Satonaka H, Nishimatsu H, Oba S, Takeda R, Omata M, Fujita T, Nagai R, Hirata Y. Myocyte enhancer factor 2 mediates vascular inflammation via the p38-dependent pathway. Circ Res 2004;95:42–49. [PubMed: 15178640]
18. Bultman, S.; Magnuson, T. Classical Genetics and Gene Targeting. In: Joyner, AL., editor. Gene targeting: A practical approach. New York: Oxford University Press Inc; 2000. p. 258-260.

19. Sundaram M, Cook HW, Byers DM. The MARCKS family of phospholipid binding proteins: regulation of phospholipase D and other cellular components. Biochem Cell Biol 2004;82:191–200. [PubMed: 15052337]
20. Faulkner G, Lanfranchi G, Valle G. Telethonin and other new proteins of the Z-disc of skeletal muscle. IUBMB Life 2001;51:275–282. [PubMed: 11699871]
21. Flower DR. The lipocalin protein family: structure and function. Biochem J 1996;318:1–14. [PubMed: 8761444]
22. Yndestad A, Landrø L, Ueland T, Dahl CP, Flo TH, Vinge LE, Espevik T, Frøland SS, Husberg C, Christensen G, Dickstein K, Kjekshus J, Øie E, Gullestad L, Aukrust P. Increased systemic and myocardial expression of neutrophil gelatinase-associated lipocalin in clinical and experimental heart failure. Eur Heart J 2009;30:1229–1236. [PubMed: 19329498]
23. Rothermel BA, Vega RB, Williams RS. The role of modulatory calcineurin interacting proteins in calcineurin signaling. Trends Cardiovasc Med 2003;13:15–21. [PubMed: 12554096]
24. Harrison BC, Kim MS, van Rooij E, Plato CF, Papst PJ, Vega RB, McAnally JA, Richardson JA, Bassel-Duby R, Olson EN, McKinsey TA. Regulation of cardiac stress signaling by protein kinase d1. Mol Cell Biol 2006;26:3875–3888. [PubMed: 16648482]
25. Hardt SE, Sadoshima J. Glycogen synthase kinase-3beta: a novel regulator of cardiac hypertrophy and development. Circ Res 2002;90:1055–1063. [PubMed: 12039794]
26. Sugden PH, Fuller SJ, Weiss SC, Clerk A. Glycogen synthase kinase 3 (GSK3) in the heart: a point of integration in hypertrophic signalling and a therapeutic target? A critical analysis. Br J Pharmacol 2008;153:S137–S153. [PubMed: 18204489]
27. Wilkins BJ, Molkentin JD. Calcium-calcineurin signaling in the regulation of cardiac hypertrophy. Biochem Biophys Res Commun 2004;322:1178–1191. [PubMed: 15336966]
28. Freeman K, Lerman I, Kranias EG, Bohlmeyer T, Bristow MR, Lefkowitz RJ, Iaccarino G, Koch WJ, Leinwand LA. Alterations in cardiac adrenergic signaling and calcium cycling differentially affect the progression of cardiomyopathy. J Clin Invest 2001;107:967–974. [PubMed: 11306600]
29. Rajabi M, Kassiotis C, Razeghi P, Taegtmeyer H. Return to the fetal gene program protects the stressed heart: a strong hypothesis. Heart Fail Rev 2007;12:331–343. [PubMed: 17516164]
30. Antos CL, McKinsey TA, Frey N, Kutschke W, McAnally J, Shelton JM, Richardson JA, Hill JA, Olson EN. Activated glycogen synthase-3 beta suppresses cardiac hypertrophy in vivo. Proc Natl Acad Sci U S A 2002;99:907–912. [PubMed: 11782539]
31. Matsuda T, Zhai P, Maejima Y, Hong C, Gao S, Tian B, Goto K, Takagi H, Tamamori-Adachi M, Kitajima S, Sadoshima J. Distinct roles of GSK-3alpha and GSK-3beta phosphorylation in the heart under pressure overload. Proc Natl Acad Sci U S A 2008;105:20900–20905. [PubMed: 19106302]
32. Chen X, Shevtsov SP, Hsich E, Cui L, Haq S, Aronovitz M, Kerkelä R, Molkentin JD, Liao R, Salomon RN, Patten R, Force T. The beta-catenin/T-cell factor/lymphocyte enhancer factor signaling pathway is required for normal and stress-induced cardiac hypertrophy. Mol Cell Biol 2006;26:4462–4473. [PubMed: 16738313]
33. Qu J, Zhou J, Yi XP, Dong B, Zheng H, Miller LM, Wang X, Schneider MD, Li F. Cardiac-specific haploinsufficiency of beta-catenin attenuates cardiac hypertrophy but enhances fetal gene expression in response to aortic constriction. J Mol Cell Cardiol 2007;43:319–326. [PubMed: 17673255]

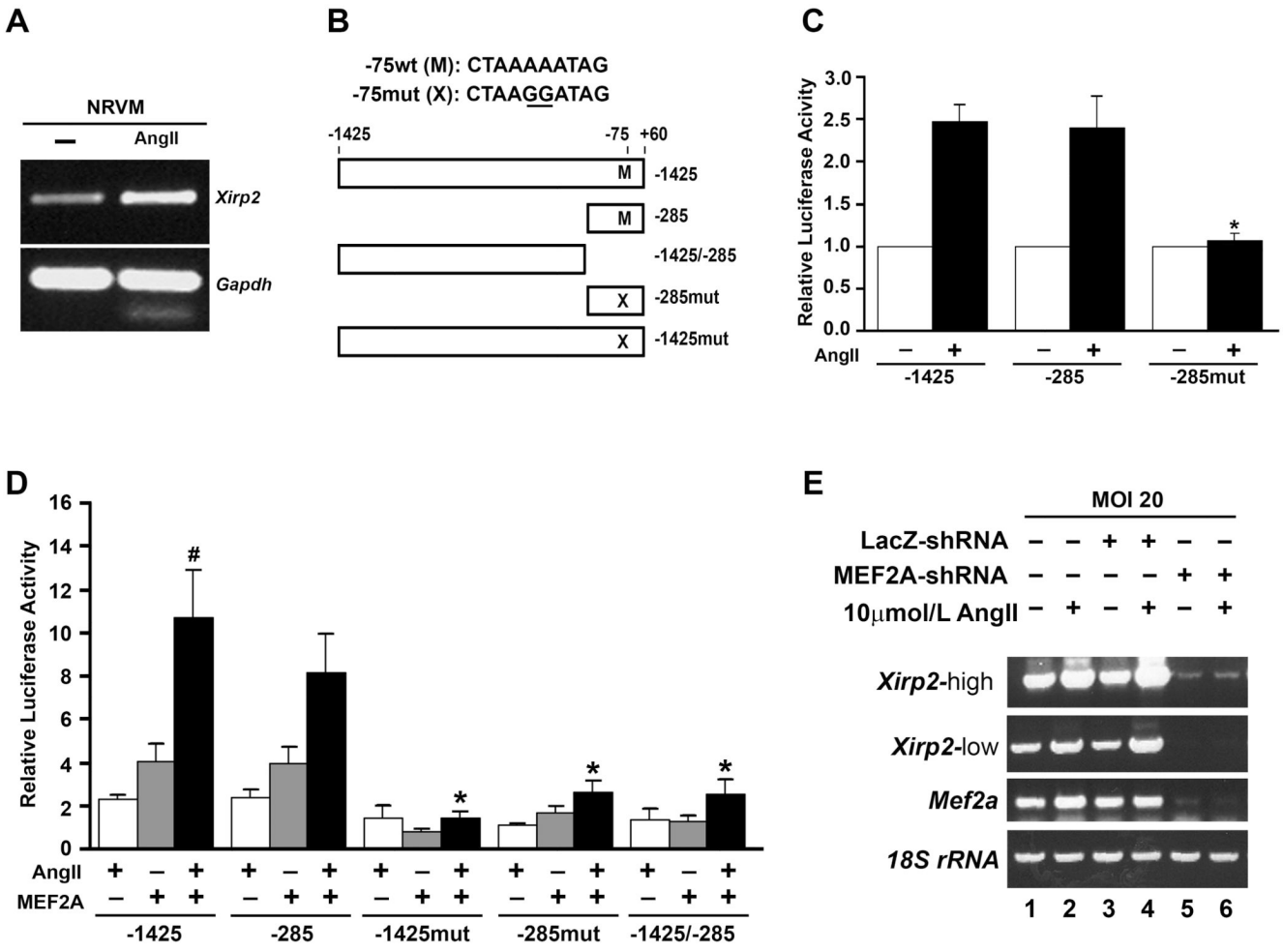

Figure 1. AngII regulates the Xirp2 promoter through MEF2A

(A) *Xirp2* RT-PCR, 10μmol/L AngII-treated NRVMs (upper panel), 2 pooled samples each, GAPDH internal control (lower panel). **(B)** *Xirp2* promoter constructs used in luciferase reporter assays. "M" denotes −75 MEF2 site, "X" denotes mutated −75 MEF2 site, sequences of wild type (M) and mutant (X) −75 MEF2 sites. **(C)** −1425 and −285 *Xirp2* promoter constructs upon 10μmol/L AngII stimulation (2.5-fold, 2.4-fold respectively) vs. basal activity. −285 construct with AngII vs. −285mut with AngII (2.4-fold vs. 1.1-fold respectively, *p<0.05). **(D)** −1425 promoter co-transfected with MEF2A and AngII vs. MEF2A alone (10.6-fold vs. 3.4-fold respectively, #p<0.05). MEF2A/AngII activation of the −1425 promoter induced to similar levels in the −285 promoter construct (8.1-fold) but significantly reduced in the −1425mut (1.4-fold, *p<0.05), −285mut (2.6-fold, *p<0.05) and the −1425/−285 (2.5-fold, *p<0.05) promoters. Luciferase data represents triplicate wells, at least 3 experimental replicates. **(C,D)** Error bars represent ±1SEM. **(E)** RT-PCR analysis in NRVMs transduced with MEF2A-shRNA or LacZ-shRNA adenoviruses in presence/absence of 10μmol/L AngII treatment. "*Xirp2-high*" and "*Xirp2-low*" are the same gel imaged at 2 different exposures. MOI, multiplicity of infection.

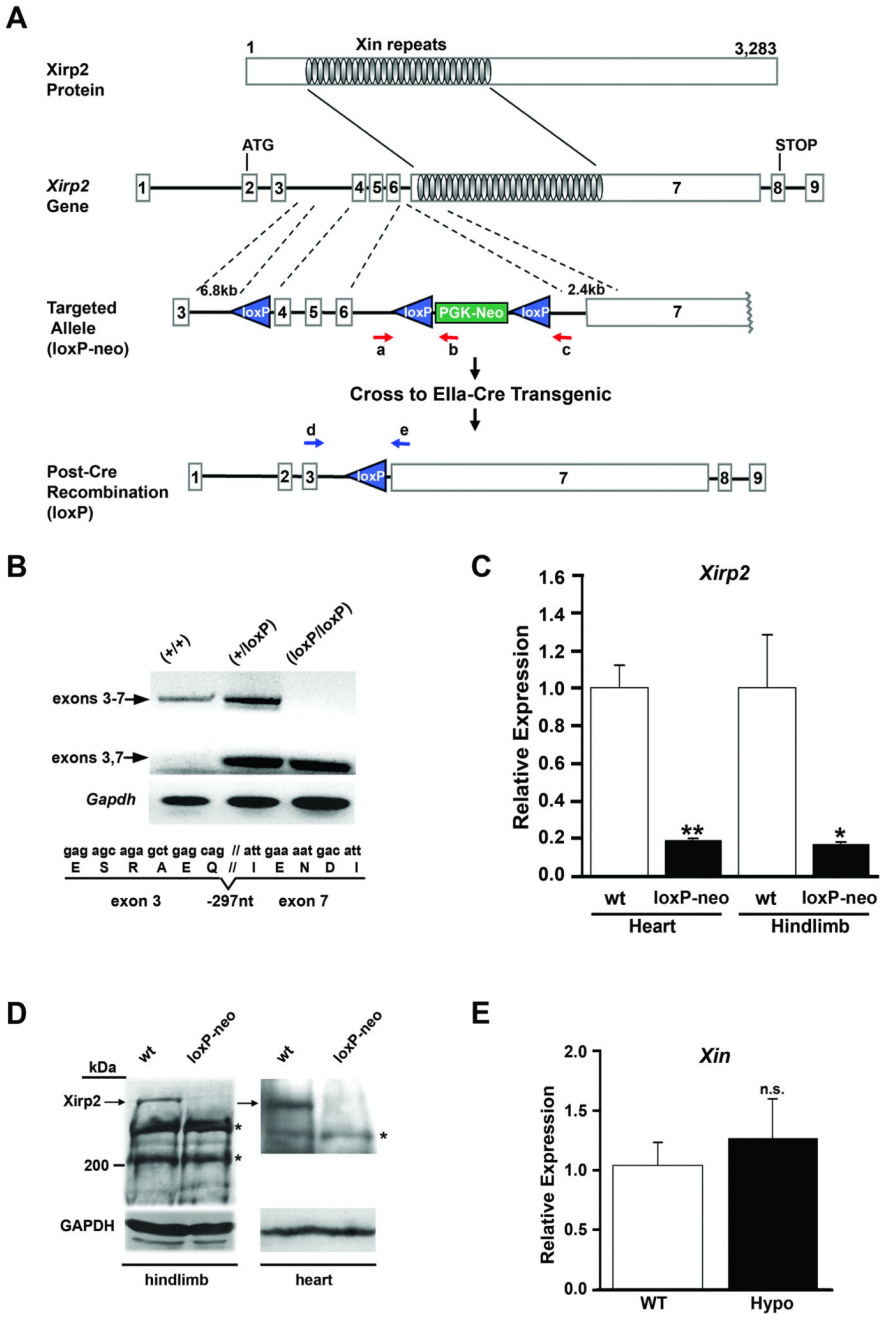

Figure 2. Targeting strategy of *Xirp2* gene and *Xirp2* hypomorphic allele

(A) Conditional targeting of the *Xirp2* gene. Genotyping primers for wt (a+c) and targeted loxP-neo (a+b). **(B)** RT-PCR on cardiac cDNA with primers (d+e). Normal transcript (exons 3–7) in wt (+/+), normal and truncated (exons 3,7) product in heterozygote (+/loxP), and truncated product in (loxP/loxP) mice. Sequencing truncated (exons 3,7) product reveals an in-frame splice. **(C)** *Xirp2* qRT-PCR with primers spanning exons 2/3. loxP-neo/loxP-neo vs. wt expression in heart (19%, **p<0.005) and skeletal muscle (17%, *p<0.05), n=3 wt, n=9 loxP-neo/loxP-neo, *B2M* internal control, results representative of multiple experiments. **(D)** Xirp2 Western blot (>360kDa top band), hindlimb (left panel) and cardiac (right panel) muscle extracts, 20μg protein/lane, (*) indicates cross-reactivity with Xin isoforms

described previously (11). **(E)** *Xin* qRT-PCR, loxP-neo/loxP-neo (Hypo) hearts vs. wt (n.s., $p>0.05$), n=3 wt, n=3 hypo, *B2M* internal control. **(C, E)** Error bars indicate ±1SEM.

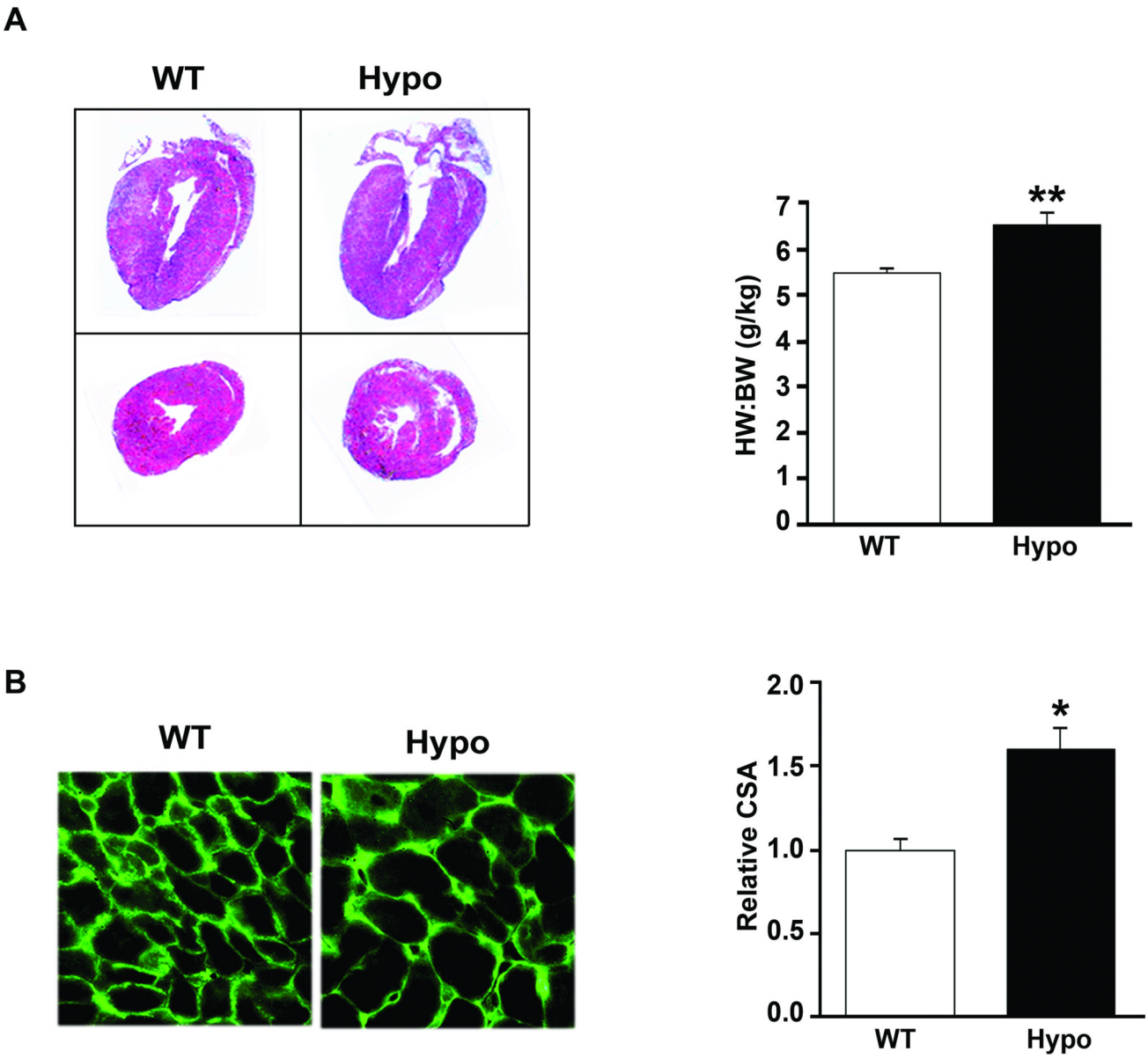

Figure 3. Unstressed *Xirp2* hypomorphic mice display cardiac hypertrophy

(A) H&E-stained heart sections (left panel) of wt and hypomorphic (hypo) mice. HW:BW (right panel), 19% increase in hypo vs. wt (ages 9–15 weeks) (**p<0.005), n=6 wt, n=14 hypo. Mean BW for wt and hypo: 22.4g and 22.3g, respectively. **(B)** Anti-vinculin immunostained ventricular myocytes (left panel). 1.6-fold increase in hypo CSA (*p<0.05), n=3 wt, n=3 hypo, 3 images/animal, ~100 myocytes/image. **(A,B)** Error bars indicate ±1SEM.

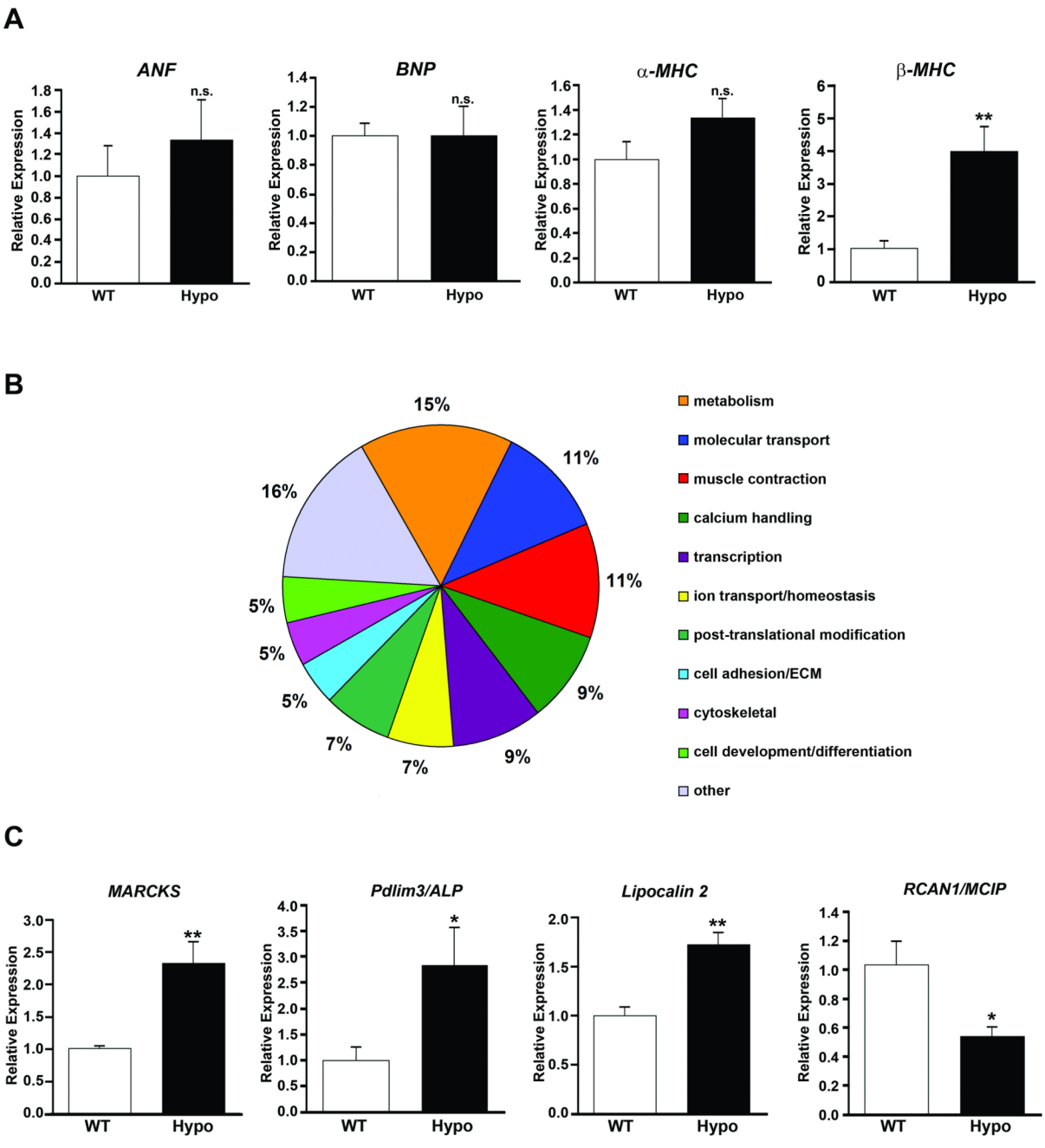

Figure 4. Global dysregulation of *Xirp2* hypomorphic cardiac gene expression

(A) qRT-PCR analysis, hypo vs. wt *ANF*, *BNP*, and α*MHC* expression (n.s., p>0.05). Hypo vs. wt β*MHC* expression (4-fold, *p<0.005), n=3 to 8 per group. **(B)** Functional categories of genes dysregulated 2-fold or greater in microarray analysis (hypo vs. wt). **(C)** qRT-PCR of selected genes from microarray. Hypo vs. wt *MARCKS* (2.3-fold, **p<0.005), *Pdlim3/ALP* (2.8-fold, *p<0.05), *Lipocalin2* (1.7-fold, **p<0.005), and *RCAN1/MCIP1* (0.5-fold, *p<0.05). n=4 to 8 per group. **(A,C)** Data representative of multiple experiments, error bars indicate ±1SEM.

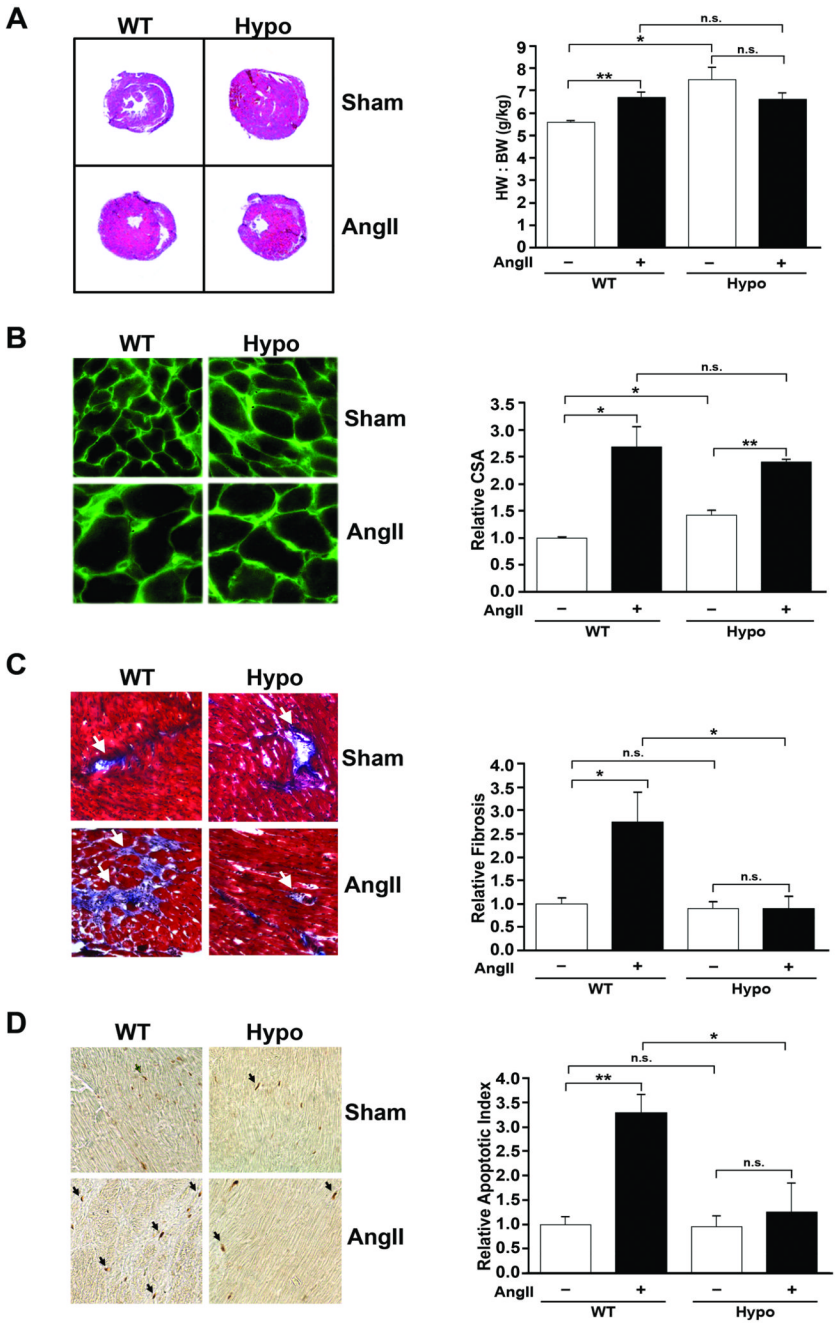

Figure 5. Attenuated response to AngII-induced cardiac remodeling in *Xirp2* hypomorphic mice

(A) H&E staining (left panel). HW:BW (right panel), AngII-wt vs. sham-wt, 20% increase (**p<0.005), AngII-hypo vs. sham-hypo (n.s., p>0.05), n=4 sham-wt, n=3 sham hypo, n=8 AngII-wt, n=6 AngII-hypo. **(B)** Anti-vinculin immunostained cardiac sections (left panel). CSA quantification (right panel), AngII-wt vs. sham-wt CSA (2.7-fold,*p<0.05), AngII-hypo vs. sham-hypo (1.7-fold,**p<0.005), n=3 to 4 per group, 3 images/animal, ~100 cardiomyocytes/image. **(C)** Masson's trichrome staining (left panel), arrows indicate fibrotic lesions. Quantification (right panel), AngII-wt vs. sham-wt (2.8--fold,*p<0.05), AngII-hypo vs. sham-hypo (n.s., p>0.05), AngII-wt vs. AngII-hypo (*p<0.05), n=3 to 5 per group, ~20 images/animal. **(D)** TUNEL-assay (left panel), arrows indicate apoptotic nuclei.

Quantification (right panel), AngII-wt vs. sham-wt (3.3-fold,**p<0.005), AngII-hypo vs. sham-hypo (n.s., p>0.05), AngII-wt vs. AngII-hypo (*p<0.05), n=3 to 4 per group, ~100 images/animal. **(A–D)** Error bars indicate ±1SEM.

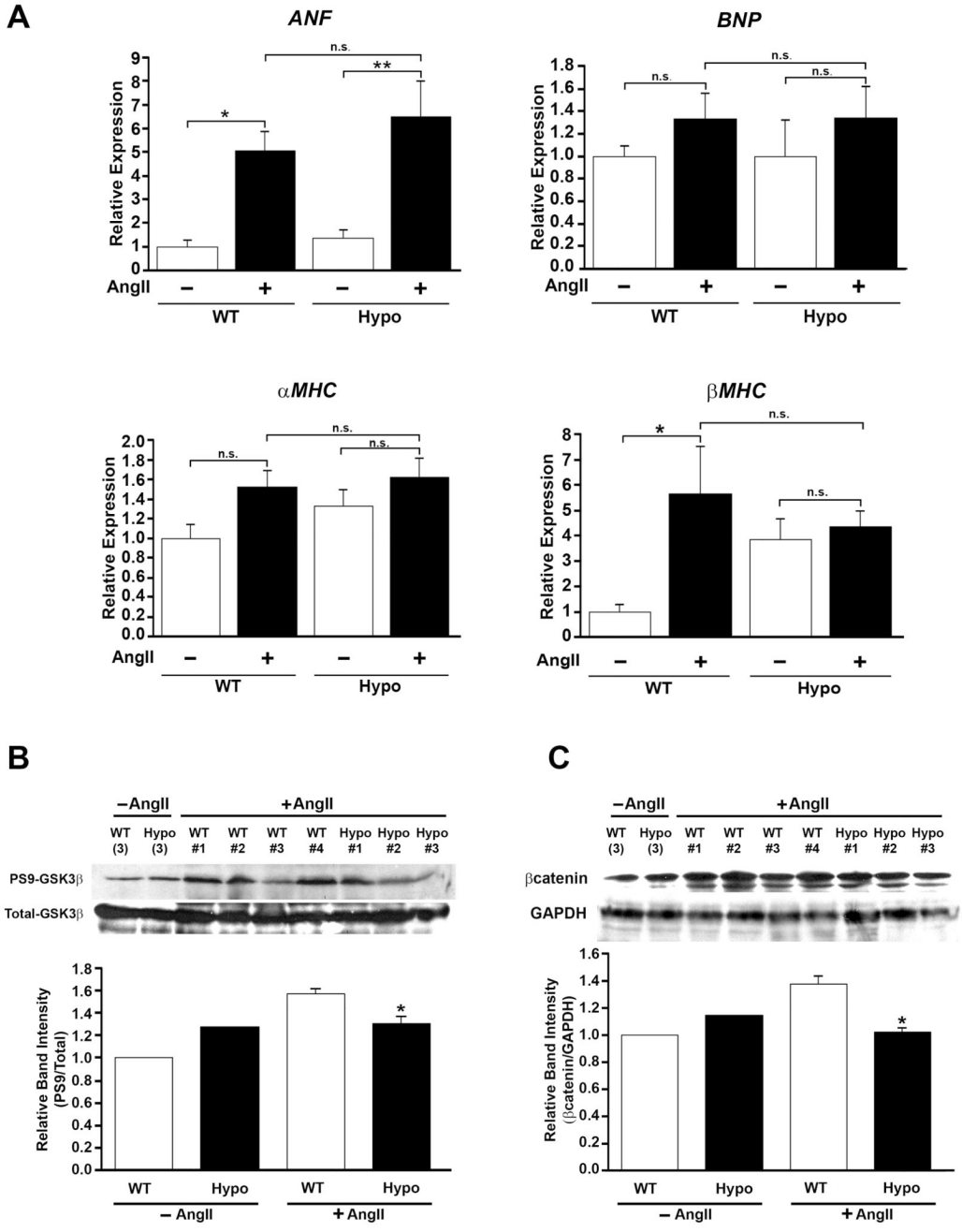

Figure 6. Expression of hypertrophic marker genes in AngII-infused hypomorphic mice

(A) qRT-PCR analysis, *ANF* expression in AngII-wt vs. wt (5.1-fold, *p<0.05) and in AngII-hypo vs. hypo (6.5-fold, *p<0.05), (n.s., p>0.05). *BNP* and α*MHC* expression (n.s., p>0.05). β*MHC* expression in AngII-wt vs. wt (5.7-fold, *p<0.05), AngII-hypo vs. hypo (n.s., p>0.05). *B2M* internal control, expression relative to untreated wt average, n=3 to 8 per group, results representative of multiple experiments. **(B)** Western blot, total and phospho-serine-9 (PS9)GSK-3β. Wt (pooled, n=3), hypo (pooled n=3), individual AngII-wt (n=4) and individual AngII-hypo (n=3) cardiac samples. Band-intensity quantified with Image-J, PS9-GSK-3β (upper blot) normalized to total GSK-3β (lower blot), AngII-hypo vs. AngII-wt (1.3-fold vs. 1.6-fold, *p<0.05). **(C)** Western blot, β-catenin levels in wt (pooled, n=3), hypo

(pooled n=3), and individual AngII-wt (n=4) and AngII-hypo (n=3) cardiac samples. Band-intensity quantified with Image-J, β-catenin (upper blot) normalized to GAPDH (lower blot), AngII-hypo vs. AngII-wt (1.0-fold vs. 1.4-fold, *$p<0.05$). **(B,C)** Relative band intensity calculated relative to wt. **(A–C)** Error bars indicate ±1SEM.